



A cysteine protease inhibitor GC376 displays potent antiviral activity against coxsackievirus infection

Yongkang Chen^{a,1}, Xiaohong Li^{a,1}, Min Wang^{a,1}, Yuan Li^a, Jun Fan^a, Jingjing Yan^a, Shuye Zhang^{b,*}, Lu Lu^{a,*}, Peng Zou^{a,*}

^a Shanghai Institute of Infectious Disease and Biosecurity, Key Laboratory of Medical Molecular Virology (MOE/NHC/CAMS), School of Basic Medical Sciences, Shanghai Public Health Clinical Center, Fudan University, Shanghai, China

^b Clinical Center for BioTherapy and Institutes of Biomedical Sciences, Zhongshan Hospital, Fudan University, Shanghai, China

ARTICLE INFO

Keywords:

Coxsackievirus
Cysteine protease
3C protease
Protease inhibitor
Antiviral
GC376

ABSTRACT

Infection with coxsackievirus A10 (CV-A10) can cause hand-foot-mouth disease and is also associated with severe complications, including viral pneumonia, aseptic and viral meningitis. Coxsackievirus infection may also play a role in the pathogenesis of acute myocardial infarction and in the increased risk of type 1 diabetes mellitus in adults. However, there are no approved vaccines or direct antiviral agents available to prevention or treatment of coxsackievirus infection. Here, we reported that GC376 potently inhibited CV-A10 infection in different cell lines without cytotoxicity, significantly suppressed production of viral proteins, and strongly reduced the yields of infectious progeny virions. Further study indicated that GC376, as viral 3C protease inhibitor, had the potential to restrain the cleavage of the viral polyprotein into individually functional proteins, thus suppressed the replication of CV-A10. Furthermore, the drug exhibited antiviral activity against coxsackieviruses of various serotypes including CV-A6, CV-A7 and CV-A16, suggesting that GC376 is a broad-spectrum anti-coxsackievirus inhibitor and the 3C protease is a promising target for developing anti-coxsackievirus agents.

Introduction

Coxsackievirus is one of the non-enveloped RNA viruses, and its infection can cause hand-foot-mouth disease (HFMD), posing a serious threat to the health of children worldwide, especially those less than 5 years old (Chen et al., 2017; Guo et al., 2022). The coxsackievirus infection may also play a direct role in the pathogenesis of acute myocardial infarction or increasing the risk of type 1 diabetes mellitus in adults (Andréoletti et al., 2007; Nekoua et al., 2022a; Nekoua et al., 2022b). In addition, infection with coxsackievirus A10 (CV-A10) is associated with severe complications including aseptic and viral meningitis (Bian et al., 2019; Cui et al., 2020). Recently, several epidemiological studies reveal that more and more HFMD cases are related to CV-A10 infection (Jiang et al., 2021; Duan et al., 2022). Moreover, CV-A10 often cocirculated with other enteroviruses, such as enterovirus A71 (EV-A71), CV-A16 and CV-A6 (Mirand et al., 2012; Zhang et al., 2015; Chen et al., 2019). However, there are no approved direct antiviral agents available to treatment with CV-A10 infection.

As a member of the genus *Enterovirus*, CV-A10 shares many characteristics with other enteroviruses. The genome of the viruses in this genus is a positive-sense single-stranded RNA, which is approximately 7.4 kbases long and contains a single open reading frame (ORF). The ORF encodes a large polyprotein that is conceptually subdivided into P1, P2 and P3 regions (Li et al., 2020). P1 encodes four structural proteins VP1-VP4, which compose the viral capsid responsible for binding to the receptor on the cells. P2 and P3 encode seven non-structural proteins 2A-2C and 3A-3D respectively, which are essential for enteroviruses replication (Saarinen et al., 2020). The enterovirus protease 3C, cleaving both viral and host proteins, participates in multiple steps of the viral lifecycle and pathological processes of the infection (M. Liu et al., 2021). As a cysteine protease, 3C cleaves the viral polyprotein to produce the separate structural and nonstructural proteins, supporting viral capsid assembly and viral RNA replication/translation cycle (Saarinen et al., 2020).

Previous studies revealed that GC376, as a covalent inhibitor against main protease (Mpro, also called 3C-like protease) of several

* Corresponding authors.

E-mail addresses: shuye_zhang@fudan.edu.cn (S. Zhang), lul@fudan.edu.cn (L. Lu), zoupeng@shphc.org.cn (P. Zou).

¹ These authors contributed equally to this work.

coronaviruses, potently restricted the infection of feline infectious peritonitis virus (FIPV) (Kim et al., 2013), severe acute respiratory syndrome coronavirus (SARS-CoV) (Kim et al., 2012) and SARS-CoV-2 (Fu et al., 2020). GC376 also suppressed the infection of noroviruses, human hepatitis A virus (HAV), human rhinovirus (HRV) and porcine teschovirus (PTV) as 3C protease inhibitor (Kim et al., 2012). In this study, the efficacy of GC376 in inhibiting infection of coxsackievirus was investigated. It was found that GC376 effectively blocked the infection of CV-A10 in different cell lines with little cytotoxicity. And the drug greatly suppressed the expression of the viral proteins and the generation of progeny infectious virions. Further investigation indicated that GC376 effectively inhibited the activity of CV-A10 3C protease, thus significantly suppressed the replication of CV-A10. Moreover, it potently inhibited infection of other serotypes of coxsackieviruses *in vitro*, such as CV-A6, CV-A7 and CV-A16. In summary, these results demonstrated that GC376, as a 3C protease inhibitor, has a potential to be developed as an antiviral agent against coxsackievirus infection.

Materials and methods

Cells, viruses, compounds and antibodies

RD cells (Human Rhabdomyosarcoma cells), Vero cells (African green monkey kidney cells) and HEK-293T cells (human embryonic kidney cells) were cultured in Dulbecco's modified Eagle's medium (DMEM; Biological Industries, Israel) supplemented 10% fetal bovine serum (FBS; Biological Industries, Israel) and 1% penicillin/streptomycin (Biological Industries, Israel) at 37 °C with 5% CO₂. Coxsackievirus A10 (CV-A10), Coxsackievirus A6 (CV-A6), Coxsackievirus A7 (CV-A7) and Coxsackievirus A16 (CV-A16) were all propagated in RD cells as described previously (Liu et al., 2021). The GC376 sodium was purchased from Targetmol (Wellesley Hills, MA, USA) at a purity of 98% and was dissolved in DMSO. The anti-3A mouse monoclonal antibody and the anti-3AB rabbit polyclonal antibody were purchased from Youke Biotech (Shanghai, China) and GeneTex (Irvine, CA, USA), respectively. The anti-GAPDH mouse monoclonal antibody was purchased from Transgen Biotech (Beijing, China).

Plaque assay

The titer of coxsackievirus was determined on RD cells by plaque assay as previously described with some modifications (Wang et al., 2020). Briefly, RD cells were seeded into 6 or 12-well cell culture plates. After culturing overnight to form confluent monolayer, the cells were infected with serially diluted viruses for 1 h. Then the inoculum was removed and immediately replaced with DMEM containing 1.2% Avicel (FMC Biopolymer, Philadelphia, PA, USA) and 2% FBS. The RD cells were further cultured at 37 °C for 2 to 3 days, then fixed and stained by 4% formaldehyde and 0.5% crystal violet respectively. Finally, plaques were counted using plaque forming unit (PFU).

Antiviral activity assays

For testing the efficacy of GC376 against coxsackievirus, RD or Vero cells were infected with CV-A10 at MOI of 0.5 or 1, respectively. After incubation of 1 h, the supernatants were replaced with fresh DMEM containing different concentrations GC376 and 2% FBS. Then the supernatant was collected at 24 or 48 h after infection respectively, and the titer of CV-A10 was determined by plaque assay as described above.

The plaque reduction assay was also performed. Briefly, the confluent RD or Vero cells seeded in cell culture plates were infected with coxsackievirus for 1 h. Then the supernatants were replaced by DMEM containing different concentration GC376, 1.2% Avicel and 2% FBS. After incubation for 2 to 3 days, the plaque was fixed and stained as described above and the half-maximal inhibitory concentrations value (IC₅₀) was calculated.

Western blot assay

RD or HEK-293T cells were infected with CV-A10 at MOI of 0.5 for 1 h, and then the supernatants were removed and immediately replaced with DMEM containing 2% FBS and serially diluted GC376. After incubation for another 10 h, the cells were collected and lysed for western blot assay to detect 3A and 3AB protein of CV-A10. Briefly, proteins in each sample were separated by SDS-polyacrylamide gel electrophoresis (SDS-PAGE), followed by being transferred to the nitrocellulose membrane. Subsequently, the membrane was blocked by 5% skim milk for 2 h and incubated with primary antibodies overnight at 4 °C. Then the membrane was incubated with horseradish peroxidase (HRP)-conjugated secondary antibodies (Dako, Glostrup, Denmark) after washing away the unbound primary antibodies. Protein bands were detected by ultrasensitive ECL chemiluminescence detection kits. The GAPDH was used as control.

Immunofluorescence staining assay

The RD cells (2×10^5 /well) seeded on coverslips in a 24-well plate were infected with CV-A10 at MOI of 2 for 1 h at 37 °C. The inoculum was replaced by fresh DMEM with different concentrations of GC376 and 2% FBS. After 8 h, cells were fixed, permeabilized and blocked by 4% paraformaldehyde, 0.2% Triton X-100 and 3% BSA (Amresco, Solon, OH, USA), respectively. After that, RD cells were incubated with mouse anti-3A primary antibodies (1:1000 dilution) for 1 h and with anti-mouse IgG conjugated to AlexaFluor488 (Jackson ImmunoResearch, West Grove, PA, USA) for another 40 min following 3 washes with PBS. After extensive washes, the coverslips were stained and sealed by Prolong Gold Antifade reagent containing DAPI (Thermo Fisher Scientific, Waltham, MA, USA) and scanned with a Leica TCS SP5 II confocal microscope.

Cell viability assays

RD, Vero or HEK-293T cells (2×10^4 /well) were seeded into 96-well cell culture plates and cultured overnight. Subsequently, the cells were incubated with fresh DMEM in the presence of serially diluted GC376 and 2% FBS. After culturing 48 h at 37 °C, cell viability was detected by Cell Counting Kit-8 (CCK8, Dojindo, Japan) as previously described (Chen et al., 2022; Wang et al., 2022).

Time-of-addition assay

The time-of-addition experiment was performed as previously described with minor modifications (Cao et al., 2021). RD cells seeded in 12-well plate were infected with CV-A10 at MOI of 2. The inoculum was discarded and fresh medium was supplemented after the cells were washed twice to remove the unbound virus at 2 h post-infection (hpi). Meanwhile, GC376 (5 μM) was added at 0, 1, 2, 4, 6, and 8 hpi until the collection of the supernatant at 12 hpi. The titer of CV-A10 particles in the supernatant was determined by plaque assay as described above.

Viral entry, attachment, internalization and post-entry assays were performed as previously described (Tan et al., 2017; Chen et al., 2019; Wang et al., 2019; Liu et al., 2020). For the entry assay, infection of RD cells with CV-A10 was accompanied by the treatment of 5 μM of GC376 at 37 °C, and then unbound viruses and drug were removed by washing with DMEM twice 1 h later. In the attachment experiment, RD cells were infected with CV-A10 in the presence of 5 μM of GC376 at 4 °C for 1 h, followed by removing unbound viruses and drugs by washing with DMEM twice. For the internalization assay, RD cells were infected with CV-A10 at 4 °C for 1 h to allow virus adsorption and then washed twice with cold DMEM to remove unbound viruses. Subsequently, RD cells were transferred to 37 °C to allow virus internalization in the presence of 5 μM of GC376, and GC376-containing medium was removed 1 h later. The overlay medium of plaque assay for viral entry, attachment and

internalization contained no GC376. In the post-entry experiment, RD cells were infected with CV-A10 at 37 °C for 1 h to allow viral entry. Subsequently, the inoculum was replaced with overlay medium containing 5 µM of GC376, 1.2% Avicel and 2% FBS. After incubation for 2 to 3 days, plaques were visualized and counted as described above.

Transient viral subgenomic replicon assay and replicon-derived single round infectious particles-based assay

Transient CV-A10 subgenomic replicon RNA transfection experiment was performed as previously described to show whether GC376 suppressed the replication of CV-A10 (Mounce et al., 2017; Wang et al., 2020). Briefly, the *in vitro* transcribed CV-A10 subgenomic replicon RNA, in which the viral structure genes (P1 region) was substituted by the luciferase reporter, was transfected into RD cells by Lipofectamine 3000 (Life Technologies, Carlsbad, USA), followed by treatment with 5 or 0.5 µM of GC376. After 24 h of incubation, the luciferase activity of the RD cell lysate was detected by luciferase assay kits (Promega, Madison, WI, USA).

The single round infectious particles (SRIPs) of CV-A10 were generated by transfection of HEK 293T cells with the capsid expresser and the CV-A10 replicon subgenomic RNA bearing the luciferase reporter as previously described (Wang et al., 2020). The SRIPs-containing inoculums were applied to RD cells seeded in 96-well culture plates at 37 °C, and then replaced by fresh DMEM with 2% FBS and GC376 (5 or 0.5 µM) 2 h later. After incubation for 24 h, the luciferase activity of the RD cell lysate was detected as described above.

CV-A10 3C protease hydrolysis activity assay

The *Escherichia coli* (E. coli) codon optimized DNA sequence of CV-A10 3C protease was synthesized in Tsingke Biotechnology and cloned into the NcoI and XhoI site of pET-28a vector, with a 6×His-tag at the C-terminus. The protein substrate MBP (Maltose Binding Protein)-TATVQGPSLD-EGFP (Enhanced Green Fluorescent Protein)-His₆, which contained the 3C protease cleavage site (TATVQGPSLD) in between MBP and EGFP, was also constructed in the NcoI and XhoI site of pET-28a by overlapping PCR and seamless cloning method. Then the two plasmids were transformed into E. coli BL21 (DE3) cells, and individual colonies were cultured in LB medium at 37 °C. The LB culture medium was then supplemented with isopropyl-β-D-1-thiogalactopyranoside (IPTG) to induce protein expression. E. coli cells were harvested by centrifugation at 7000 rpm for 10 min after 16 h of culturation at 18 °C, and resuspended in lysis buffer (100 mM Tris-HCl, 400 mM NaCl, pH 8.0). Subsequently, cells were crushed in an ultrasonic cell pulverizer (SCIENITZ-1200E, Ningbo Scientz Biotechnology, Ningbo, China) and centrifuged at 12,500 g for 20 min. Next, the supernatant was added to Ni Sepharose 6 Fast Flow (GE Healthcare Bio-Sciences, Sweden). The target protein was eluted with the buffer containing 100 mM Tris-HCl, 150 mM NaCl and 250 mM imidazole (pH 8.0) after the resin was thoroughly washed with wash buffer (100 mM Tris-HCl, 800 mM NaCl, 30 mM imidazole, pH 8.0). The purified protein was dialyzed against 50 mM Tris-HCl, 150 mM NaCl (pH 8.0) at 4 °C and stored at -20 °C.

The inhibition of GC376 on the hydrolytic activity of CV-A10 3C protease was then evaluated by cleavage of MBP-TATVQGPSLD-EGFP-His₆. The 3C protease were incubated with MBP-TATVQGPSLD-EGFP and GC376 (10, 1 or 0.1 µM) in the buffer containing 50 mM Tris-HCl, 150 mM NaCl and 1 mM DTT (pH 8.0) at 30 °C for 4 h, and then the cleavage of MBP-TATVQGPSLD-EGFP was visualized by SDS-PAGE and Coomassie brilliant blue staining.

Statistical analysis

One-way ANOVA was utilized to compare the inhibitory activity of different concentration GC376 on the yields of CV-A10 and the replication of CV-A10 replicon RNA. Student's unpaired two-tailed *t*-test was

employed to examine the antiviral activities of GC376 on CV-A10 entry, attachment, internalization and post-entry between the DMSO group and GC376 group. Statistical analyses were carried out by GraphPad Prism Software 7.0 (GraphPad Prism Software Inc., CA, USA). NS, not significant; * *p* < 0.05; ** *p* < 0.01; *** *p* < 0.001; and **** *p* < 0.0001.

Results

GC376 inhibits coxsackievirus A10 infection in different cell lines

To explore the inhibitory effects of GC376 against coxsackievirus A10 (CV-A10) infection, a plaque reduction assay was performed. RD cells were infected with CV-A10 at 37 °C for 1 h, and then the inoculum was replaced by overlay medium containing serially diluted GC376. As shown in Fig. 1A, the plaque numbers gradually decreased with the increasing concentrations of GC376, demonstrating that GC376 effectively inhibited the infection of CV-A10 in a dose-dependent manner. The half-maximal inhibitory concentrations (IC₅₀) value of GC376 against CV-A10 in plaque reduction assay was 0.24 ± 0.04 µM (Fig. 1B).

We next assessed whether treatment with GC376 would restrict the expression of viral proteins and reduce the yields of progeny virus particles. RD cells were infected by CV-A10 at MOI of 0.5 for 1 h. Subsequently, the supernatants were replaced by overlay medium containing 2% FBS and different concentrations of GC376. The RD cells or supernatants were collected at 10 or 24 h post-infection (hpi), respectively. As shown in Fig. 1C, GC376 at the concentration of 0.63 µM had little inhibitory activity on the expression of the viral 3A protein, while 2.5 µM of GC376 completely blocked the viral protein expression following infection with CV-A10. In addition, the titer of CV-A10 in the supernatant was determined on RD cells by plaque assay. We found that the yields of infectious virions were also significantly reduced by 1.47 Log₁₀ (96.61%), 3.61 Log₁₀ (99.98%) and 5.26 Log₁₀ (~100.00%) with 1.1, 3.3 and 10 µM of GC376 compared to DMSO control, respectively (Fig. 1D). Taken together, these data indicated that GC376 greatly reduced the viral protein expression and the generation of infectious virus particles in RD cells following CV-A10 infection, suggesting that GC376 exhibited potent antiviral activity against CV-A10 *in vitro*.

To further confirm the suppression activity of GC376 against CV-A10, we conducted an immunofluorescence assay to detect the expression of viral 3A protein following CV-A10 infection at higher MOI (MOI of 2). Treatment with 3.3 µM GC376 also strongly inhibited the viral 3A protein expression. Moreover, the percentage of infected-RD cells decreased by more than 50% when treated with 1.1 µM of GC376 (Fig. 2), which was in accordance with the above results.

To investigate whether GC376 effectively blocked CV-A10 infection in other cell lines, the plaque reduction assay was also performed on Vero cells. As shown in Fig. 3A, GC376 also significantly inhibited CV-A10 infection in a dose-dependent manner with IC₅₀ values of 1.69 ± 0.62 µM. Furthermore, Vero cells were also infected with CV-A10 at MOI of 1 to determine whether GC376 restricted the yield of progeny infectious CV-A10. As expected, we did observe the decrease of viral yield in the GC376-treated groups. The titers of progeny CV-A10 virions were reduced by 66.45%, 85.65% and 96.84% when treated with 1.1, 3.3 and 10 µM of GC376, respectively (Fig. 3B). Besides, 1 µM of GC376 significantly restricted viral 3AB protein expression in HEK-293T cells infected with CV-A10 at MOI of 0.5 (Fig. 3C). Meanwhile, GC376 exhibited low cytotoxicity to RD (Fig. 3D), Vero (Fig. 3E) and HEK-293T cells (Fig. 3F). Collectively, these results confirm that GC376 has potent and lasting inhibitory activity on CV-A10 infection in various cell lines with low cytotoxicity.

GC376 inhibits CV-A10 infection in the late stage

To elucidate the potential antiviral mechanism of GC376 against CV-A10 infection, a time-of-addition assay was conducted to identify which stage of the virus life cycle was blocked by the drug. As illustrated in

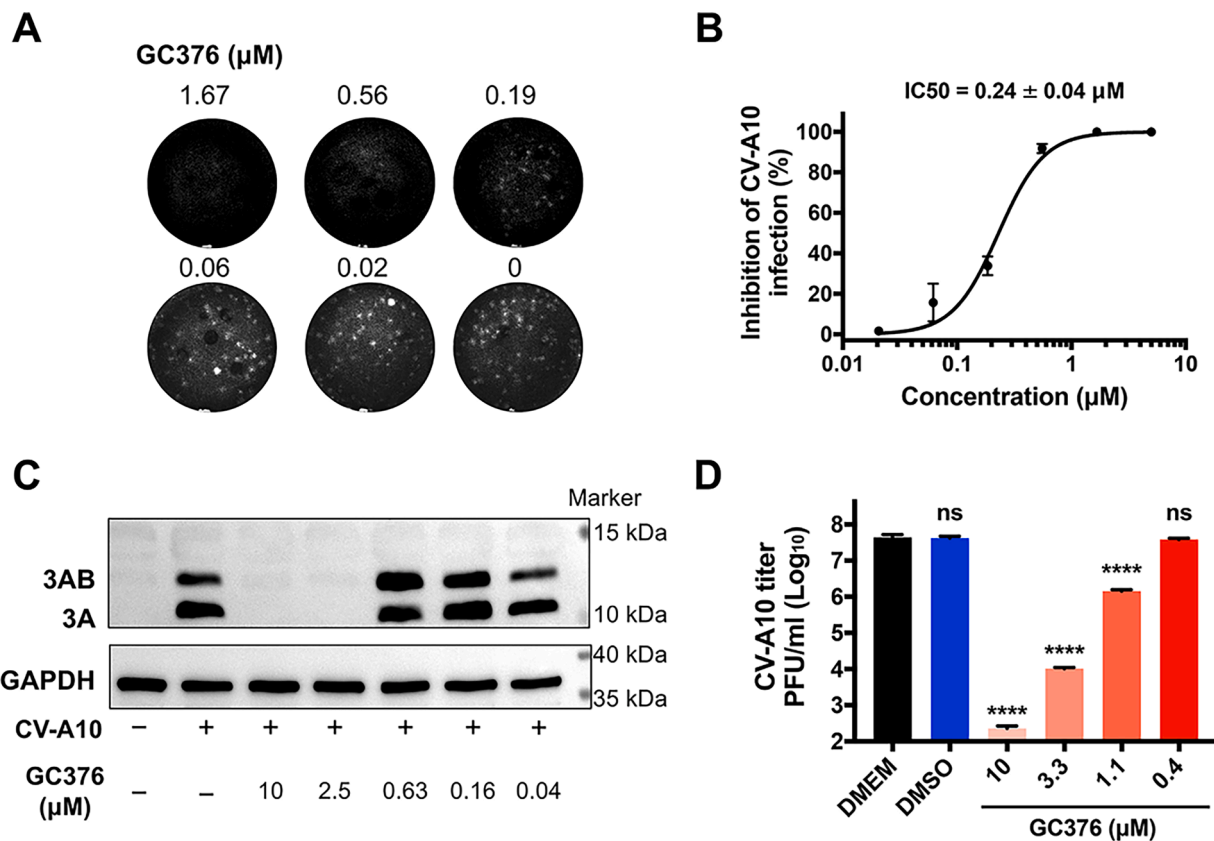


Fig. 1. The inhibitory activity of GC376 against CV-A10 infection in RD cells. (A) Antiviral effects of GC376 against CV-A10 infection was measured by plaque reduction assay and IC₅₀ value was calculated (B). GC376 suppressed the expression of viral 3A proteins (C) and the yields of progeny virions (D) following CV-A10 infection. Data are represented as means ± SD. NS, not significant; **** $p < 0.0001$.

Fig. 4A, the RD cells were infected with CV-A10 and the viruses were removed 2 hpi by washing with fresh DMEM. GC376 (5 μM) was added at the indicated time points and the yields of CV-A10 in the supernatants at 12 hpi were measured by plaque assays. As shown in Fig. 4B, the CV-A10-infected RD cells shrank, became round and lost normal morphology, exhibiting cytopathic effect (CPE) compared to the uninfected control, while addition of GC376 at 0, 1, 2 and 4 hpi potently inhibited the CPE induced by virus infection and reduced the yields of the progeny CV-A10 (Fig. 4C). Moreover, addition of GC376 at 6 hpi still significantly suppressed the production of progeny virions by more than 60%. These results demonstrated that addition of the drugs in the late stage of CV-A10 infection could still inhibit the proliferation of the virus.

Next, viral entry and post-entry experiments were carried out to further confirm at which particular step GC376 exhibited antiviral properties against CV-A10 infection. As shown in Fig. 4D (I), 5 μM of GC376 and CV-A10 were simultaneously incubated with RD cells at 37 °C for 1 h, and drug and unbound viruses were then removed by washing with fresh DMEM, followed by plaque assay. However, no significant differences were observed between GC376-treated and DMSO groups. The results suggest that GC376 treatment might not disturb the entry step of CV-A10 infection. In support of this, viral attachment and internalization assays were performed as previously described. As expected, GC376 did not block attachment or internalization of CV-A10 (Fig. 4D II and III), while GC376 could significantly inhibit CV-A10 infection after the viruses had entered into the cells (Fig. 4D IV). Taken together, these results suggest that GC376 is a post-entry inhibitor against CV-A10.

GC376 effectively suppresses the replication of CV-A10 RNA by blocking proteolytic activity of CV-A10 3C protease

The viral subgenomic replicon system and replicon-based single round infectious particles (SRIPs) with the viral structural genes (P1 region) replaced by luciferase reporter are safe and useful tools to evaluate inhibitor activities which inhibit viral RNA replication (Xie et al., 2016; Wang et al., 2020). In order to further assess that whether GC376 could suppress CV-A10 viral RNA replication as a post-entry inhibitor, CV-A10 SRIPs with luciferase reporter were utilized. RD cells seeded in 96-well culture plate were infected with CV-A10 SRIPs for 2 h, followed by removal of the inoculum and adding fresh medium containing different concentrations of GC376. After culturing for 24 h, the luciferase activity was detected. As shown in Fig. 5A, upon the treatment with GC376 at 5 μM, the luciferase activities significantly decreased by 2.47 Log₁₀ (99.66%), demonstrating that GC376 effectively suppressed CV-A10 viral RNA replication in RD cells. Similarly, 5 μM of GC376 also exhibited potent inhibitory activity against the replication of the CV-A10 subgenomic RNA which was transcribed from replicon plasmid *in vitro* and then directly transfected into RD cells (Fig. 5B).

It was reported that GC376 is a cysteine protease covalent inhibitor that potently restricts the infection of human hepatitis A virus, human rhinovirus, enterovirus A71, and some coronaviruses including feline infectious peritonitis virus, SARS-CoV and SARS-CoV-2 (Kim et al., 2012; Kim et al., 2013; Fu et al., 2020). The 3C protease of CV-A10 is also a cysteine protease which plays an important role in the hydrolysis of coxsackievirus polyprotein and consequently converting it into separate proteins with different functions. Therefore, we questioned whether GC376 could act as a 3C cysteine protease inhibitor to suppress the replication of CV-A10. Thus, the inhibitory effect of GC376 on

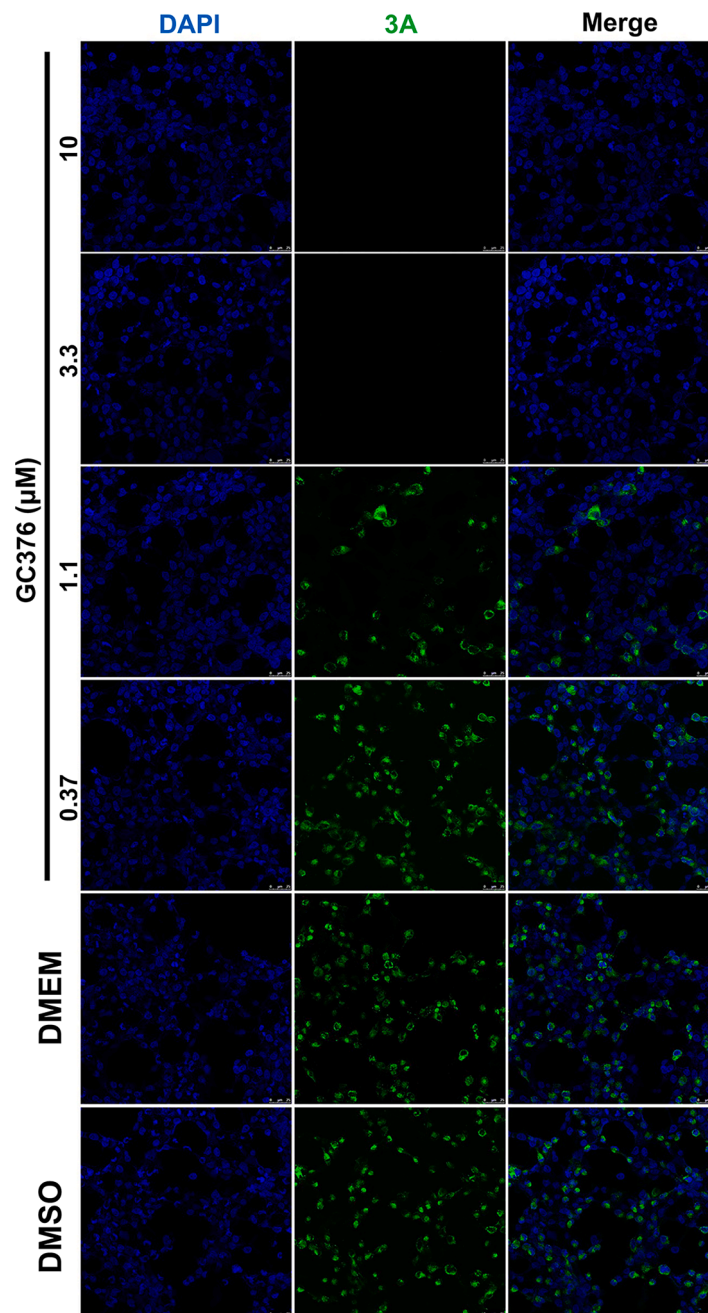


Fig. 2. GC376 effectively restrained viral protein expression in CV-A10 infected-RD cells. RD cells were infected by CV-A10 at a multiplicity of infection (MOI) of 2, and then treated with serially diluted GC376. After 8 h of cultivation, viral 3A proteins expressed in the cells were stained by anti-3A mouse monoclonal antibody (green); nuclei were stained by 4,6-diamidino-2-phenylindole (DAPI, blue). Scale bar: 25 μm .

CV-A10 3C protease hydrolyzing a protein substrate (MBP-TATVQGPSLD-EGFP-His₆), which contained the protease cleavage site TATVQGPSLD, was assessed. As shown in Fig. 6, the SDS-PAGE results showed that the MBP-TATVQGPSLD-EGFP protein were hydrolyzed to MBP and EGFP by CV-A10 3C protease *in vitro*, and GC376 blocked the activity of 3C protease in a dose-dependent manner, suggesting that GC376 exhibited antiviral efficacy by restraining the hydrolysis of the polyprotein by CV-A10 3C protease.

GC376 inhibits infection of various serotypes of coxsackieviruses

CV-A10 often co-circulates with other coxsackieviruses, such as CV-A16 and CV-A6 (Mirand et al., 2012; Zhang et al., 2015; Chen et al., 2019). Thus, in order to identify whether GC376 exhibited

broad-spectrum anti-coxsackievirus activities, the plaque reduction assay was performed using coxsackieviruses of different serotypes. The results indicated that GC376 significantly inhibited the infection of CV-A16, CV-A6 and CV-A7 in a dose dependent manner, with IC₅₀ values of $0.18 \pm 0.02 \mu\text{M}$ (Fig. 7A), $0.22 \pm 0.02 \mu\text{M}$ (Fig. 7B) and $0.21 \pm 0.05 \mu\text{M}$ (Fig. 7C), respectively. These results demonstrated that GC376 possessed significant antiviral activities against coxsackieviruses of various serotypes, suggesting GC376 is a broad-spectrum anti-coxsackievirus inhibitor.

Discussion

The genomic RNA of the positive-sense RNA viruses, such as coronavirus, enterovirus and flavivirus, can serve as the messenger RNA that

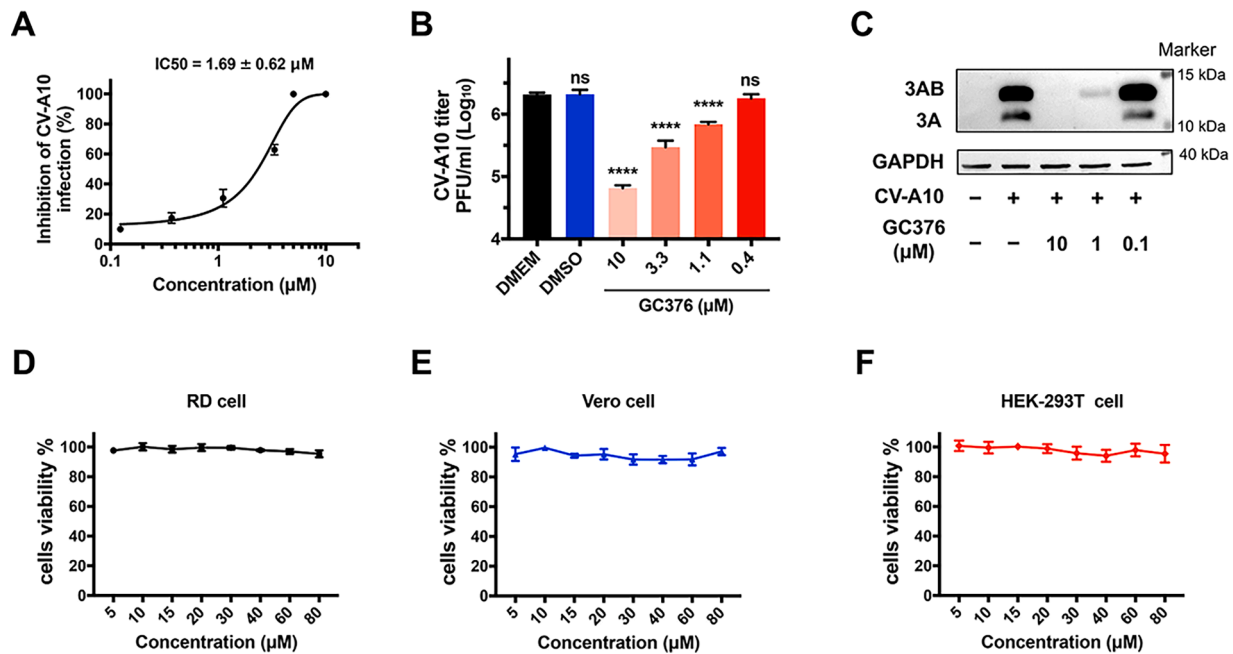


Fig. 3. The inhibitory activity of GC376 against CV-A10 infection in Vero and HEK-293T cells and its toxicity to these cell lines. (A) Anti-CV-A10 effects of GC376 was measured by plaque reduction assay in Vero cells. (B) GC376 significantly inhibited the yield of progeny virions in Vero cells infected by CV-A10. (C) GC376 restricted viral 3A proteins expression in HEK-293T cells following CV-A10 infection at MOI of 0.5. The RD (D), Vero (E) and HEK-293T cells (F) were treated with different concentrations of GC376, and the cell viability was detected by Cell Counting Kit-8. Data are represented as means \pm SD. NS, not significant; **** $p < 0.0001$.

is directly translated to a large precursor protein usually called polyprotein, making the function of virus encoded protease a prerequisite for proper proteolytic processing of the polyprotein that is necessary for virus replication. The protease can be released from the polyprotein by autocleavage and then split the polyprotein into some smaller structural and nonstructural proteins in specific site. Some of the virus encoded proteases are serine protease for flavivirus and HIV, while others are cysteine protease for coronavirus and enterovirus, etc. The cysteine protease encoded by enterovirus or coxsackievirus is called 3C protease, which is responsible for cleavage of the polyprotein. Interestingly, accumulating evidence indicated that 3C protease can be involved in the cleavage of host proteins to resist host immune response (Lei et al., 2011; Lei et al., 2013; Xiang et al., 2016; Xiao et al., 2021). For example, interferon regulatory factor 7 (IRF7) suppresses virus infection, while EV-A71 3C protease cleaves IRF7 to inhibit its function, thus escaping cellular responses (Lei et al., 2013). Moreover, 3C protease exhibits activity of cleaving the Toll-like receptors pathway ligand TRIF, therefore inhibiting the production of IFN- β and the activation of NF- κ B (Lei et al., 2011).

Given its essential roles in viral replication and infection, more and more viral protease inhibitors have been developed for clinic use or are under studies. The inhibitors against serine protease of HIV, together with reverse transcriptase inhibitors, have constituted the regime of highly active antiretroviral therapy (HAART) to achieve HIV virological suppression. Beside non-competitive or non-covalent inhibitors (Ratia et al., 2008; Xu et al., 2021; Liang et al., 2022), small molecule compounds covalently linked to thiol group have also been discovered because of the high nucleophilicity of thiol group on cysteine residue located in the catalytically active site of cysteine protease (Dai et al., 2020; Liu et al., 2021). Paxlovid, a drug under investigation which consists of covalent coronavirus cysteine protease inhibitor (nirmatrelvir) and an enhancer (ritonavir) has been authorized for the emergency use to treat mild-to-moderate COVID-19. Recently, besides the enterovirus A71, infections by coxsackieviruses of different serotypes are reported increasingly to cause HFMD outbreaks. However, infection by one coxsackievirus confers no or little cross-protection against

infection by other serotypes, and there are no approved antiviral agents available to treatment with coxsackievirus infection. Although GC376 has been previously reported to inhibit 3C or 3C-like proteases of some viruses, its effects on coxsackievirus infection have not been characterized in detail and whether GC376 has broad-spectrum anti-coxsackievirus properties also needs to be clarified.

In this study, the results showed that GC376 could effectively suppress coxsackievirus replication, which may be attributed to multiple mechanisms. First, the viral proteins involved in coxsackievirus RNA replication become mature only after being cleaved by 3C protease and released from the polyprotein encoded by coxsackievirus itself. For example, the 3B protein, a small nonstructural protein commonly known as viral protein genome-linked protein (VPg), serves as primer for viral RNA synthesis when uridylylated by viral 3D polymerase and covalently linked to the 5' termini of the viral RNAs (Paul et al., 1998; Pathak et al., 2007; Gruez et al., 2008). The 3D protein, a viral RNA-dependent RNA polymerase (RdRp), is responsible for chain elongation during viral RNA replication. The RdRp activity of 3D is obscured in its precursor 3CD and restored when separated from 3C by autocleavage of 3C protease between 3C carboxy-terminus and 3D amino-terminus (Harris et al., 1992). Other viral nonstructural proteins participated in the replication complex formation, such as 2B, 2C and 3A, also need to be proteolytically cleaved and released from polyprotein by 3C. On the other hand, 3C protease cleaves cellular proteins involved in the interferon pathway to antagonize the inhibition of viral RNA replication (Lei et al., 2013). Hence, as the specific inhibitor of coxsackievirus 3C protease, GC376 could impede the maturation of viral proteins important for viral RNA replication and relieve the repression of IFN pathway, resulting in the inhibition of replication of viral RNA in host cells.

In conclusion, GC376 was demonstrated to exert potent efficacy to inhibit CV-A10 infection in different cell lines. It interfered with the proteolytic processing of CV-A10 polyprotein by blocking the activity of CV-A10 3C protease, hence suppressed viral RNA replication. Moreover, GC376 exhibited antiviral activity against various serotypes of coxsackieviruses, indicating that the 3C protease of coxsackievirus is indeed a promising target for developing anti-coxsackievirus agents with broad-

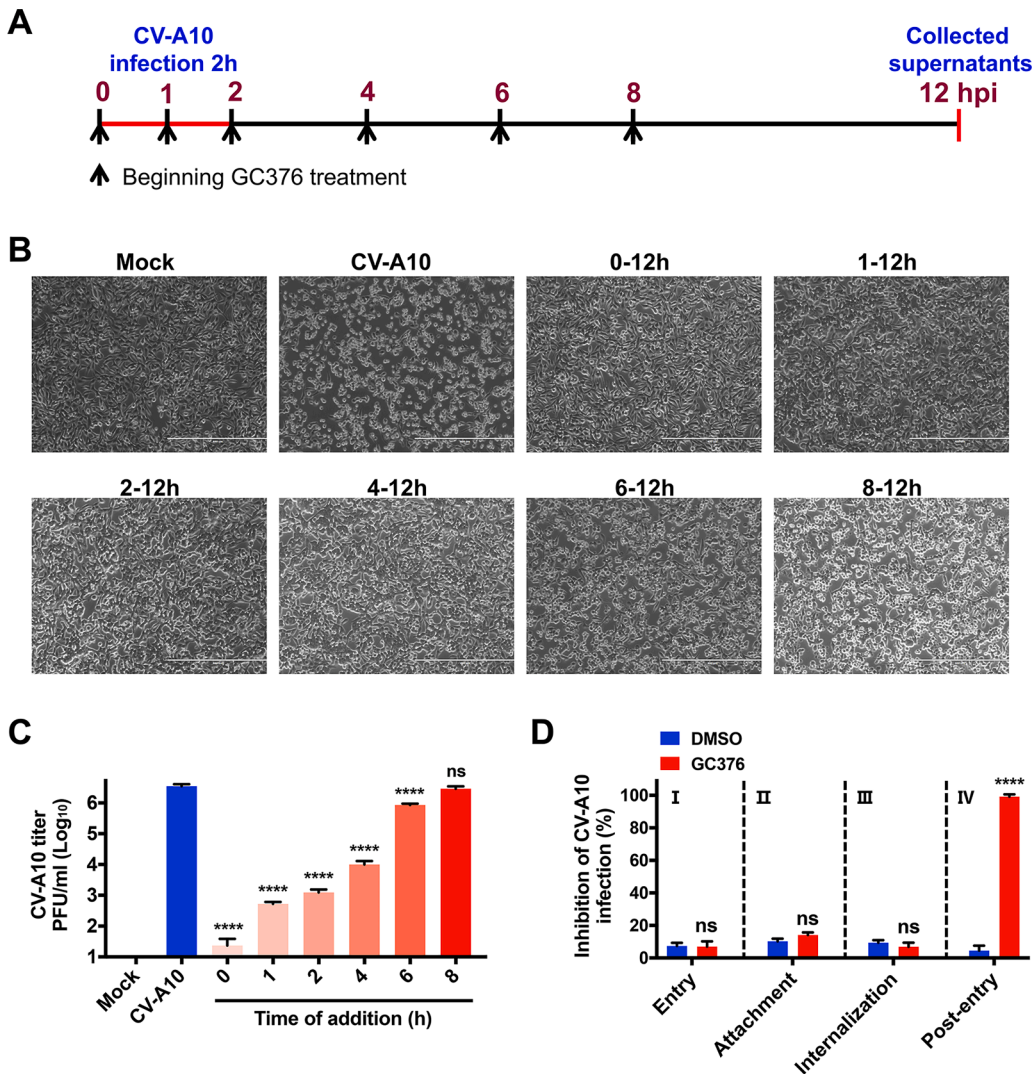


Fig. 4. GC376 inhibited CV-A10 infection in the late stage. (A) Outline of the time-of-addition experiment that was utilized to identify at which stage the CV-A10 lifecycle was blocked by GC376. hpi means hours post infection. (B) GC376 was added at different time points as indicated, and then cytopathic effect (CPE) were observed under microscope. Scale bar: 400 μ m. (C) The virus titers in the supernatants were also measured at 12 hpi by plaque assays. (D) For the entry assay, RD cells were treated with CV-A10 and 5 μ M of GC376 at 37 $^{\circ}$ C for 1 h, and then unbound viruses and drug were removed. For the attachment assay, RD cells were infected by CV-A10 at 4 $^{\circ}$ C for 1 h in the presence of 5 μ M of GC376, followed by removing unbound viruses and drugs. For the internalization assay, RD cells were infected with CV-A10 at 4 $^{\circ}$ C for 1 h to allow virus adsorption and washed twice with cold DMEM to remove unbound viruses, and then RD cells were incubated at 37 $^{\circ}$ C for 1 h to allow virus internalization in the presence of 5 μ M of GC376, followed by removal of the drug. For the post-entry experiment, RD cells were infected with CV-A10 at 37 $^{\circ}$ C for 1 h to allow viral entry, and then the inoculum was removed. The overlay medium, supplemented with GC376 for post-entry assay or without GC376 for the other three assays, was then added to conduct plaque assay. Data are represented as means \pm SD. NS, not significant; **** $p < 0.0001$.

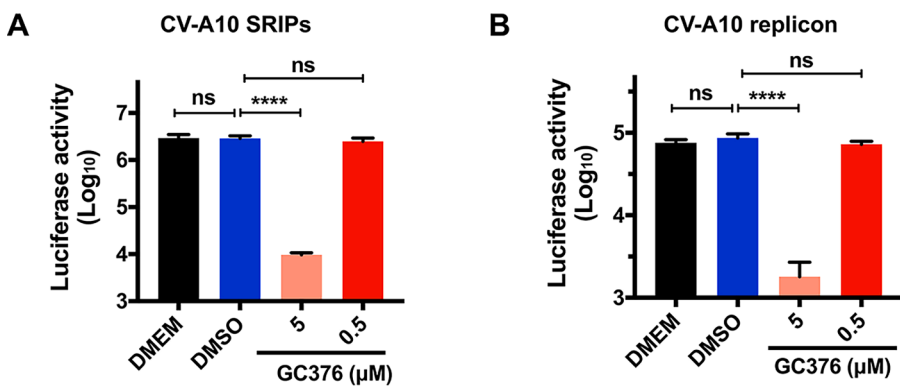


Fig. 5. GC376 potently suppressed the replication of the CV-A10 subgenomic viral RNA. (A) Single round infectious particles (SRIPs), which encapsulated the luciferase reporter gene-containing CV-A10 subgenomic RNA, was utilized to infect RD cells with or without GC376 treatment. The luciferase activity of cell lysate was detected at 24 hpi, showing the suppression of CV-A10 viral RNA replication by GC376 treatment. (B) RD cells were transfected with *in vitro* transcribed CV-A10 replicon RNA bearing luciferase reporter and simultaneously treated with GC376, followed by detection of luciferase activity of the cell lysate at 24 hpi. Data are represented as means \pm SD. NS, not significant; **** $p < 0.0001$.

spectrum activity.

Ethics statement

No human or animal subjects were involved in this study.

Funding

This work was funded by grants from Shanghai Municipal Science and Technology Major Project (ZD2021CY001), the National Natural Science Foundation of China (82172250 and 82002135), and from the Shanghai Public Health Clinical Center (KY-GW-2017-17 and KY-GW-2020-10).

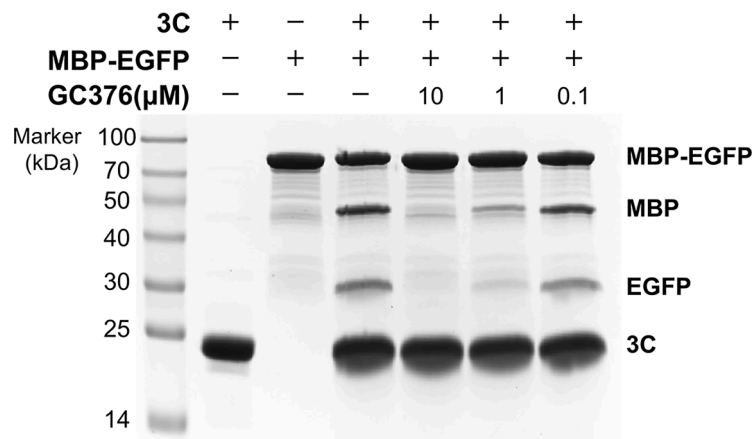


Fig. 6. GC376 effectively inhibited the proteolytic activity of CV-A10 3C protease. CV-A10 3C protease together with the MBP-TATVQGPSLD-EGFP-His6 protein, which contained the 3C protease cleavage site TATVQGPSLD as the substrate, were treated with or without GC376 at 30 °C for 4 h. Then the proteins in each sample were subsequently separated and visualized by SDS-PAGE and Coomassie brilliant blue staining.

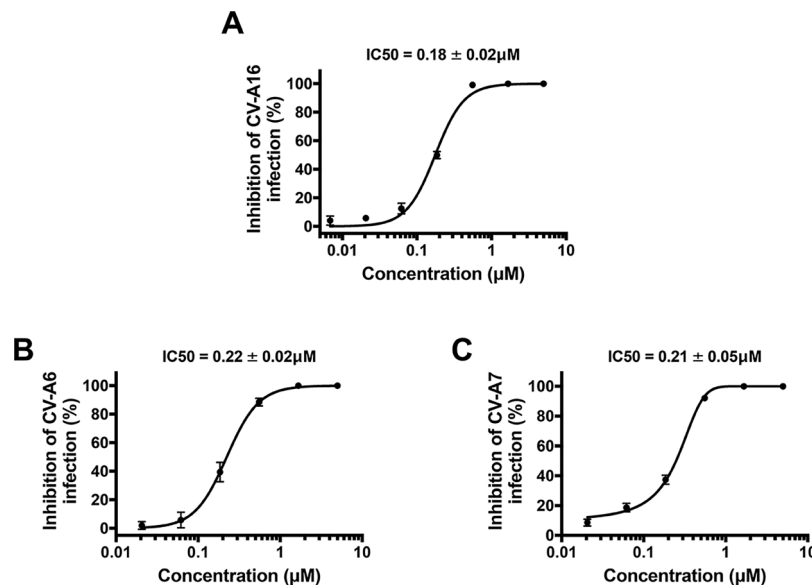


Fig. 7. The activities of GC376 against different serotypes of coxsackieviruses. Inhibitory effects of GC376 against infection of CV-A16 (A), CV-A6 (B) and CV-A7 (C) were measured by plaque reduction assay. Data are represented as means \pm SD.

CRedit authorship contribution statement

Yongkang Chen: Methodology, Validation, Formal analysis, Investigation, Data curation, Visualization, Writing – original draft, Writing – review & editing. **Xiaohong Li:** Methodology, Validation, Formal analysis, Investigation, Data curation, Writing – review & editing. **Min Wang:** Methodology, Writing – review & editing. **Yuan Li:** Methodology, Writing – review & editing. **Jun Fan:** Methodology, Writing – review & editing, Funding acquisition. **Jingjing Yan:** Methodology, Writing – review & editing. **Shuye Zhang:** Writing – review & editing, Supervision, Funding acquisition. **Lu Lu:** Conceptualization, Writing – review & editing, Supervision, Funding acquisition. **Peng Zou:** Conceptualization, Writing – review & editing, Supervision, Funding acquisition.

Declaration of Competing Interest

The authors declare that they have no known competing financial interests or personal relationships that could have appeared to influence the work reported in this paper.

Data availability

Data will be made available on request.

References

- Andréoletti, L., Ventéo, L., Douche-Aourik, F., Canas, F., Lorin De La Grandmaison, G., Jacques, J., Moret, H., Jovenin, N., Mosnier, J.F., Matta, M., Duband, S., Pluot, M., Pozzetto, B., Bourlet, T., 2007. Active Coxsackievirus B infection is associated with disruption of dystrophin in endomyocardial tissue of patients who died suddenly of acute myocardial infarction. *J. Am. Coll. Cardiol.* 50, 2207–2214. <https://doi.org/10.1016/j.jacc.2007.07.080>.
- Bian, L., Gao, F., Mao, Q., Sun, S., Wu, X., Liu, S., Yang, X., Liang, Z., 2019. Hand, foot, and mouth disease associated with coxsackievirus A10: more serious than it seems. *Expert Rev. Anti Infect. Ther.* 17, 233–242. <https://doi.org/10.1080/14787210.2019.1585242>.
- Cao, Y., Lei, E., Wang, X., Qi, X., Li, L., Ren, J., Yang, J., Wang, S., 2021. Licochalcone A inhibits enterovirus A71 replication *in vitro* and *in vivo*. *Antiviral Res.* 195, 105091. <https://doi.org/10.1016/j.antiviral.2021.105091>.
- Chen, J., Ye, X., Zhang, X.Y., Zhu, Z., Zhang, X., Xu, Z., Ding, Z., Zou, G., Liu, Q., Kong, L., Jiang, W., Zhu, W., Cong, Y., Huang, Z., 2019a. Coxsackievirus A10 atomic structure facilitating the discovery of a broad-spectrum inhibitor against human enteroviruses. *Cell Discov.* 5, 4. <https://doi.org/10.1038/s41421-018-0073-7>.

- Chen, M., He, S., Yan, Q., Xu, X., Wu, W., Ge, S., Zhang, S., Chen, M., Xia, N., 2017. Severe hand, foot and mouth disease associated with Coxsackievirus A10 infections in Xiamen, China in 2015. *J. Clin. Virol.* 93, 20–24. <https://doi.org/10.1016/j.jcv.2017.05.011>.
- Chen, Y., Li, Y., Wang, X., Zou, P., 2019b. Montelukast, an anti-asthmatic drug, inhibits zika virus infection by disrupting viral integrity. *Front. Microbiol.* 10, 3079. <https://doi.org/10.3389/fmicb.2019.03079>.
- Chen, Y., Wang, X., Shi, H., Zou, P., 2022. Montelukast inhibits HCoV-OC43 infection as a viral inactivator. *Viruses* 14. <https://doi.org/10.3390/v14050861>.
- Cui, Y., Peng, R., Song, H., Tong, Z., Qu, X., Liu, S., Zhao, X., Chai, Y., Wang, P., Gao, G. F., Qi, J., 2020. Molecular basis of Coxsackievirus A10 entry using the two-in-one attachment and uncoating receptor KRM1. *Proc. Natl. Acad. Sci. U. S. A.* 117, 18711–18718. <https://doi.org/10.1073/pnas.2005341117>.
- Dai, W., Zhang, B., Jiang, X.M., Su, H., Li, J., Zhao, Y., Xie, X., Jin, Z., Peng, J., Liu, F., Li, C., Li, Y., Bai, F., Wang, H., Cheng, X., Cen, X., Hu, S., Yang, X., Wang, J., Liu, X., Xiao, G., Jiang, H., Rao, Z., Zhang, L.K., Xu, Y., Yang, H., Liu, H., 2020. Structure-based design of antiviral drug candidates targeting the SARS-CoV-2 main protease. *Science* 368, 1331–1335. <https://doi.org/10.1126/science.abb4489>.
- Duan, S., Yang, F., Li, Y., Zhao, Y., Shi, L., Qin, M., Liu, Q., Jin, W., Wang, J., Chen, L., Zhang, W., Li, Y., Zhang, Y., Zhang, J., Ma, S., He, Z., Li, Q., 2022. Pathogenic analysis of coxsackievirus A10 in rhesus macaques. *Virol. Sin.* 37, 610–618. <https://doi.org/10.1016/j.virs.2022.06.007>.
- Fu, L., Ye, F., Feng, Y., Yu, F., Wang, Q., Wu, Y., Zhao, C., Sun, H., Huang, B., Niu, P., Song, H., Shi, Y., Li, X., Tan, W., Qi, J., Gao, G.F., 2020. Both Boceprevir and GC376 efficaciously inhibit SARS-CoV-2 by targeting its main protease. *Nat. Commun.* 11, 4417. <https://doi.org/10.1038/s41467-020-18233-x>.
- Gruez, A., Selisko, B., Roberts, M., Bricogne, G., Bussetta, C., Jabafi, I., Coutard, B., De Palma, A.M., Neyts, J., Canard, B., 2008. The crystal structure of coxsackievirus B3 RNA-dependent RNA polymerase in complex with its protein primer VPg confirms the existence of a second VPg binding site on Picornaviridae polymerases. *J. Virol.* 82, 9577–9590. <https://doi.org/10.1128/jvi.00631-08>.
- Guo, J., Cao, Z., Liu, H., Xu, J., Zhao, L., Gao, L., Zuo, Z., Song, Y., Han, Z., Zhang, Y., Wang, J., 2022. Epidemiology of hand, foot, and mouth disease and the genetic characteristics of Coxsackievirus A16 in Taiyuan, Shanxi, China from 2010 to 2021. *Front. Cell. Infect. Microbiol.* 12, 1040414 <https://doi.org/10.3389/fcimb.2022.1040414>.
- Harris, K.S., Reddigari, S.R., Nicklin, M.J., Hämmerle, T., Wimmer, E., 1992. Purification and characterization of poliovirus polypeptide 3CD, a proteinase and a precursor for RNA polymerase. *J. Virol.* 66, 7481–7489. <https://doi.org/10.1128/jvi.66.12.7481-7489.1992>.
- Jiang, H., Zhang, Z., Rao, Q., Wang, X., Wang, M., Du, T., Tang, J., Long, S., Zhang, J., Luo, J., Pan, Y., Chen, J., Ma, J., Liu, X., Fan, M., Zhang, T., Sun, Q., 2021. The epidemiological characteristics of enterovirus infection before and after the use of enterovirus 71 inactivated vaccine in Kunming, China. *Emerg. Microbes Infect.* 10, 619–628. <https://doi.org/10.1080/22221751.2021.1899772>.
- Kim, Y., Lovell, S., Tiew, K.C., Mandadapu, S.R., Alliston, K.R., Battaile, K.P., Groutas, W. C., Chang, K.O., 2012. Broad-spectrum antivirals against 3C or 3C-like proteases of picornaviruses, noroviruses, and coronaviruses. *J. Virol.* 86, 11754–11762. <https://doi.org/10.1128/jvi.01348-12>.
- Kim, Y., Mandadapu, S.R., Groutas, W.C., Chang, K.O., 2013. Potent inhibition of feline coronaviruses with peptidyl compounds targeting coronavirus 3C-like protease. *Antiviral Res.* 97, 161–168. <https://doi.org/10.1016/j.antiviral.2012.11.005>.
- Lei, X., Sun, Z., Liu, X., Jin, Q., He, B., Wang, J., 2011. Cleavage of the adaptor protein TRIF by enterovirus 71 3C inhibits antiviral responses mediated by Toll-like receptor 3. *J. Virol.* 85, 8811–8818. <https://doi.org/10.1128/jvi.00447-11>.
- Lei, X., Xiao, X., Xue, Q., Jin, Q., He, B., Wang, J., 2013. Cleavage of interferon regulatory factor 7 by enterovirus 71 3C suppresses cellular responses. *J. Virol.* 87, 1690–1698. <https://doi.org/10.1128/jvi.01855-12>.
- Li, X., Wang, M., Cheng, A., Wen, X., Ou, X., Mao, S., Gao, Q., Sun, D., Jia, R., Yang, Q., Wu, Y., Zhu, D., Zhao, X., Chen, S., Liu, M., Zhang, S., Liu, Y., Yu, Y., Zhang, L., Tian, B., Pan, L., Chen, X., 2020. Enterovirus Replication Organelles and Inhibitors of Their Formation. *Front. Microbiol.* 11, 1817 <https://doi.org/10.3389/fmicb.2020.01817>.
- Liang, J., Zheng, M., Xu, W., Chen, Y., Tang, P., Wu, G., Zou, P., Li, H., Chen, L., 2022. Acriflavine and proflavine hemisulfate as potential antivirals by targeting M(pro). *Bioorg. Chem.* 129, 106185 <https://doi.org/10.1016/j.bioorg.2022.106185>.
- Liu, L., Wang, M., Yu, R., Li, H., Fan, J., Yan, J., Liu, Z., Zhang, S., 2021a. Preparation and verification of a monoclonal antibody against a conserved linear epitope in enterovirus A protein 2C. *J. Virol. Methods* 298, 114298. <https://doi.org/10.1016/j.jviromet.2021.114298>.
- Liu, M., Xu, B., Ma, Y., Shang, L., Ye, S., Wang, Y., 2021b. Reversible covalent inhibitors suppress enterovirus 71 infection by targeting the 3C protease. *Antiviral Res.* 192, 105102 <https://doi.org/10.1016/j.antiviral.2021.105102>.
- Liu, Z., Xia, S., Wang, X., Lan, Q., Li, P., Xu, W., Wang, Q., Lu, L., Jiang, S., 2020. Sodium copper chlorophyllin is highly effective against enterovirus (EV) A71 infection by blocking its entry into the host cell. *ACS Infect. Dis.* 6, 882–890. <https://doi.org/10.1021/acinfed.0c00096>.
- Mirand, A., Henquell, C., Archimbaud, C., Ughetto, S., Antona, D., Bailly, J.L., Peigue-Lafeuille, H., 2012. Outbreak of hand, foot and mouth disease/herpangina associated with coxsackievirus A6 and A10 infections in 2010, France: a large citywide, prospective observational study. *Clin. Microbiol. Infect.* 18, E110–E118. <https://doi.org/10.1111/j.1469-0691.2012.03789.x>.
- Mounce, B.C., Cesaro, T., Carrau, L., Vallet, T., Vignuzzi, M., 2017. Curcumin inhibits Zika and chikungunya virus infection by inhibiting cell binding. *Antiviral Res.* 142, 148–157. <https://doi.org/10.1016/j.antiviral.2017.03.014>.
- Nekoua, M.P., Alidjinou, E.K., Hober, D., 2022a. Persistent coxsackievirus B infection and pathogenesis of type 1 diabetes mellitus. *Nat. Rev. Endocrinol.* 18, 503–516. <https://doi.org/10.1038/s41574-022-00688-1>.
- Nekoua, M.P., Mercier, A., Alhazmi, A., Sane, F., Alidjinou, E.K., Hober, D., 2022b. Fighting enteroviral infections to prevent type 1 diabetes. *Microorganisms*, 10. <https://doi.org/10.3390/microorganisms10040768>.
- Pathak, H.B., Arnold, J.J., Wiegand, P.N., Hargittai, M.R., Cameron, C.E., 2007. Picornavirus genome replication: assembly and organization of the VPg uridylylation ribonucleoprotein (initiation) complex. *J. Biol. Chem.* 282, 16202–16213. <https://doi.org/10.1074/jbc.M610608200>.
- Paul, A.V., Van Boom, J.H., Filippov, D., Wimmer, E., 1998. Protein-primed RNA synthesis by purified poliovirus RNA polymerase. *Nature* 393, 280–284. <https://doi.org/10.1038/30529>.
- Ratia, K., Pegan, S., Takayama, J., Sleeman, K., Coughlin, M., Baliji, S., Chaudhuri, R., Fu, W., Prabhakar, B.S., Johnson, M.E., Baker, S.C., Ghosh, A.K., Mesecar, A.D., 2008. A noncovalent class of papain-like protease/deubiquitinase inhibitors blocks SARS virus replication. *Proc. Natl. Acad. Sci. U. S. A.* 105, 16119–16124. <https://doi.org/10.1073/pnas.0805240105>.
- Saarinen, N.V.V., Stone, V.M., Hankaniemi, M.M., Mazur, M.A., Vuorinen, T., Flodström-Tullberg, M., Hyöty, H., Hytönen, V.P., Laitinen, O.H., 2020. Antibody responses against enterovirus proteases are potential markers for an acute infection. *Viruses* 12. <https://doi.org/10.3390/v12010078>.
- Tan, C.W., Sam, I.C., Chong, W.L., Lee, V.S., Chan, Y.F., 2017. Polysulfonate suramin inhibits Zika virus infection. *Antiviral Res.* 143, 186–194. <https://doi.org/10.1016/j.antiviral.2017.04.017>.
- Wang, M., Yan, J., Zhu, L., Wang, M., Liu, L., Yu, R., Chen, M., Xun, J., Zhang, Y., Yi, Z., Zhang, S., 2020. The establishment of infectious clone and single round infectious particles for coxsackievirus A10. *Virol. Sin.* 35, 426–435. <https://doi.org/10.1007/s12250-020-00198-2>.
- Wang, X., Chen, Y., Shi, H., Zou, P., 2022. Erythromycin estolate is a potent inhibitor against HCoV-OC43 by directly inactivating the virus particle. *Front. Cell. Infect. Microbiol.* 12, 905248 <https://doi.org/10.3389/fcimb.2022.905248>.
- Wang, X., Xia, S., Zou, P., Lu, L., 2019. Erythromycin estolate inhibits zika virus infection by blocking viral entry as a viral inactivator. *Viruses* 11. <https://doi.org/10.3390/v11111064>.
- Xiang, Z., Liu, L., Lei, X., Zhou, Z., He, B., Wang, J., 2016. 3C protease of enterovirus D68 inhibits cellular defense mediated by interferon regulatory factor 7. *J. Virol.* 90, 1613–1621. <https://doi.org/10.1128/jvi.02395-15>.
- Xiao, H., Li, J., Yang, X., Li, Z., Wang, Y., Rui, Y., Liu, B., Zhang, W., 2021. Ectopic expression of TRIM25 restores RIG-I expression and IFN production reduced by multiple enteroviruses 3C(pro). *Virol. Sin.* 36, 1363–1374. <https://doi.org/10.1007/s12250-021-00410-x>.
- Xie, X., Zou, J., Shan, C., Yang, Y., Kum, D.B., Dallmeier, K., Neyts, J., Shi, P.Y., 2016. Zika virus replicons for drug discovery. *EBioMedicine* 12, 156–160. <https://doi.org/10.1016/j.ebiom.2016.09.013>.
- Xu, B., Liu, M., Ma, S., Ma, Y., Liu, S., Shang, L., Zhu, C., Ye, S., Wang, Y., 2021. 4-iminoxazolidin-2-one as a bioisostere of cyanohydrin suppresses EV71 proliferation by targeting 3C(pro). *Microbiol. Spectr.* 9, e0102521 <https://doi.org/10.1128/Spectrum.01025-21>.
- Zhang, C., Zhu, R., Yang, Y., Chi, Y., Yin, J., Tang, X., Yu, L., Zhang, C., Huang, Z., Zhou, D., 2015. Phylogenetic analysis of the major causative agents of hand, foot and mouth disease in Suzhou City, Jiangsu province, China, in 2012–2013. *Emerg. Microbes Infect.* 4, e12 <https://doi.org/10.1038/emi.2015.12>.